

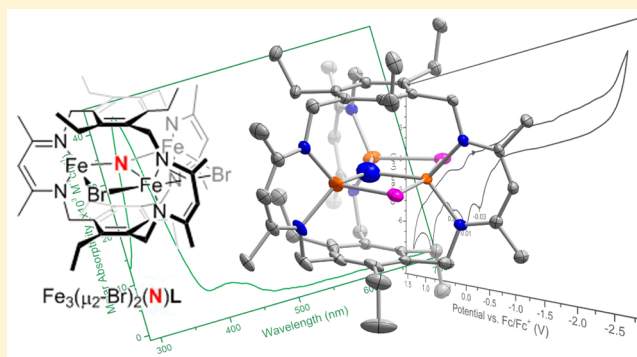
# Nitride-Bridged Triiron Complex and Its Relevance to Dinitrogen Activation

David M. Ermert, Jesse B. Gordon, Khalil A. Abboud, and Leslie J. Murray\*

Department of Chemistry, Center for Catalysis, University of Florida, Gainesville, Florida 32611, United States

**S** Supporting Information

**ABSTRACT:** Using a simple metathesis approach, the triiron(II) tribromide complex  $\text{Fe}_3\text{Br}_3\text{L}$  (**1**) reacts with tetrabutylammonium azide to afford the monoazide dibromide analogue  $\text{Fe}_3(\text{Br})_2(\text{N}_3)\text{L}$  (**2**) in high yield. The inclusion of azide was confirmed by IR spectroscopy with a  $\nu(\text{N}_3) = 2082 \text{ cm}^{-1}$  as well as combustion analysis and X-ray crystallography. Heating **2** in the solid state results in the complete loss of the azide vibration in the IR spectra and the isolation of the olive-green mononitride complex  $\text{Fe}_3(\text{Br})_2(\text{N})\text{L}$  (**3**). Solution magnetic susceptibility measurements support that the trimetallic core within **2** is oxidized upon generation of **3** (5.07 vs 3.09  $\mu_B$ ). Absorption maxima in the UV–visible–near-IR (NIR) spectra of **2** and **3** support the azide-to-nitride conversion, and a broad NIR absorption centered at 1117 nm is similar to that previously reported for the intervalence charge-transfer band for a mixed-valent nitridodiron cluster. The cyclic voltammograms recorded for **3** are comparable to those of **1** with no reductive waves observed between  $\sim 0$  and  $-2.5 \text{ V}$  (vs  $\text{Fc}/\text{Fc}^+$ ), whereas a reversible one-electron redox process is observed for  $\text{Fe}_3(\text{NH}_2)_3\text{L}$  (**4**). These results suggest that intercluster cooperativity is unlikely to predominate the dinitrogen reduction mechanism when **1** is treated with  $\text{KC}_8$  under  $\text{N}_2$ .



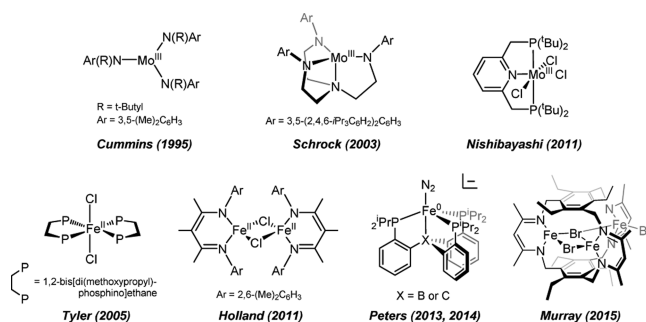
## INTRODUCTION

Although the six-electron reduction of dinitrogen to ammonia or compounds with similarly reduced N atoms [e.g.,  $(\text{Me}_3\text{Si})_3\text{N}$ ] is thermodynamically favored, the kinetic difficulties associated with this reaction are usually attributed to the larger energetic costs for transferring fewer equivalents of electrons and protons (e.g.,  $2e^-/\text{H}^+$  to form diazene).<sup>1</sup> Ammonia in particular is a chemical of great societal importance as a fertilizer and as a raw material for value-added chemical synthesis. Currently, ammonia is produced using the Haber–Bosch process, in which a potassium-doped iron catalyst facilitates the interconversion of dinitrogen and dihydrogen to ammonia at elevated temperatures and pressures.<sup>2</sup> In contrast to the high energy demands of this method, the nitrogenase enzymes catalyze the reduction of dinitrogen to ammonia using reducing equivalents derived from NADH and protons under ambient conditions. The active sites of these enzymes share a similar  $\text{Fe}_7\text{S}_9$  cluster, which is capped at one end by either a Mo, V, or Fe atom.<sup>3</sup> All forms are competent for dinitrogen activation; however, the molybdenum-containing cofactor, or  $\text{FeMoco}$ , is the most active and most investigated to date.

Stemming in part from the composition of  $\text{FeMoco}$ , one avenue of ongoing research focuses on the development of molecular molybdenum and iron complexes as catalysts for dinitrogen activation. Cummins and co-workers first reported dinitrogen cleavage by a three-coordinate molybdenum(III)

complex,<sup>4</sup> and this discovery was followed by that of the single-site molybdenum catalyst from the Schrock group (Scheme 1).<sup>5</sup> This catalyst reduces dinitrogen to ammonia under fairly mild conditions and in good yields. More recently, Nishibayashi developed mono- and dimetallic molybdenum catalysts supported by pincer-type ligands, including a recently reported complex that activates  $\text{N}_2$  upon irradiation.<sup>6</sup> Iron is the common metal to both the biological and industrial processes,

## Scheme 1



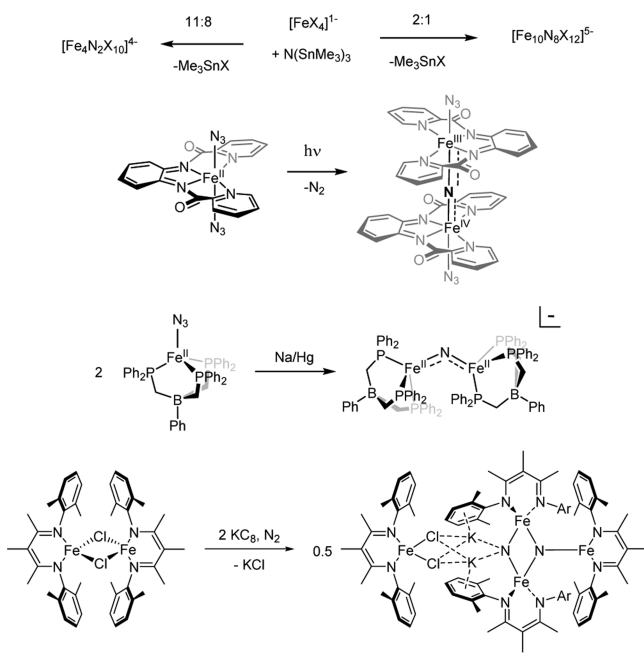
**Special Issue:** Small Molecule Activation: From Biological Principles to Energy Applications

**Received:** April 11, 2015

**Published:** June 8, 2015

implying that one or more Fe centers could react in a redox cooperative manner to cleave dinitrogen. Indeed, recent ENDOR studies have suggested that  $N_2$  binds to the tetrairon face of FeMoco after the resting cluster has been reduced by four electrons, suggesting that iron is the reactive metal center(s) for dinitrogen reduction.<sup>7</sup> Unsurprisingly then, the reactivity of dinitrogen with low-valent Fe centers has also been explored. Tyler et al. reported a mononuclear iron complex that activated dihydrogen and reduced dinitrogen to ammonia, albeit in low yields (Scheme 1).<sup>8</sup> More recently, Holland and co-workers demonstrated that chemical reduction of a ( $\beta$ -diketiminato)iron(II) complex under a dinitrogen atmosphere resulted in the cleavage of  $N_2$  to afford nitride ligands (Scheme 2).<sup>9</sup> In this system, the initial step is proposed to be

Scheme 2



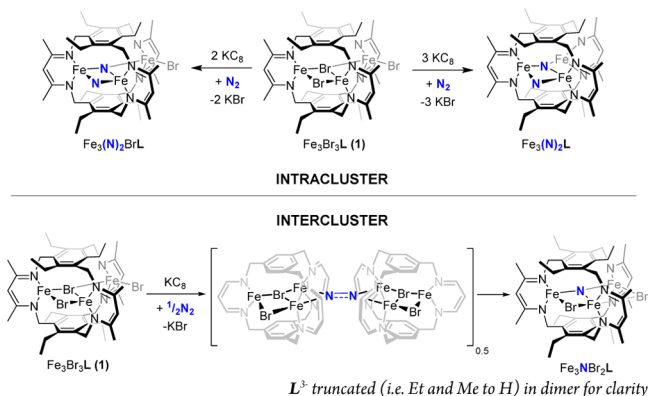
coordination of dinitrogen to either one or more iron(I) species based on DFT experiments.<sup>9</sup> The isolation of a  $M_2Fe_4(N)_2$  ( $M = K^+$  or  $Rb^+$ ) cluster as well as triiron clusters of the type  $MFe_3(N)_2$  ( $M = Na^+$  or  $K^+$ ) hints at a cooperative effect between the Fe centers and a functional role for the alkali cation.<sup>9,10</sup> In addition, the nitride ligands in these clusters were recently demonstrated to re-form dinitrogen,<sup>10a</sup> which has only been reported for one other system.<sup>6e</sup> Relatedly, the Peters group has investigated a series of trigonal-pyramidal iron compounds as catalysts for dinitrogen reduction, in which the effect of the apical donor atom on catalysis was evaluated (Scheme 1).<sup>11</sup> As a departure from the monoiron complexes, this group also reported a designed diiron complex containing two bridging hydride ligands and demonstrated a significant rate enhancement for dinitrogen coordination upon reduction to the  $Fe^I Fe^II$  state.<sup>12</sup> With the exception of this diiron example, the focus thus far has been predominantly on the reactivity of monometallic compounds with comparatively little focus on understanding how multiple metal centers act in concert to bind and cleave dinitrogen. Given that FeMoco operates at a significantly lower overpotential than the reported molecular systems, we aimed to develop a synthetic approach to understanding how redox cooperativity between multiple Fe

centers might facilitate dinitrogen reduction and possibly allow for milder reductants to be employed.

In the first reported structure of FeMoco, the central cavity of the iron–sulfur cluster was modeled as vacant without an interstitial atom.<sup>13</sup> Higher resolution data ultimately revealed the presence of a  $\mu_6$ -ligand coordinated to the six Fe atoms constituting the “iron-belt” that was initially assigned as a nitride ligand, thought to arise from the inclusion of one N atom from dinitrogen into the cluster during catalytic turnover.<sup>14</sup> Recently, however, a detailed analysis of the X-ray diffraction and absorption data in addition to  $^{14}C$ -labeling studies provided strong evidence for an interstitial carbide ligand in FeMoco.<sup>15</sup> The discussion of the identity of the central atom resulted in an interest in understanding how the central atom type influences the properties of molecular clusters,<sup>16</sup> including dinitrogen reduction and coordination, and how those results could inform the reaction mechanism of FeMoco. Somewhat relatedly, transient intermediates containing nitride bridges are proposed computationally during the nitrogenase catalytic cycle, and these transients differentiate the distal and alternating mechanisms.<sup>14,15,17</sup> Expectedly, both mono- and polynuclear iron nitride complexes have been synthesized and their redox properties and reactivities investigated. Typically, nitride-bridged polyiron clusters have been synthesized by decomposition of coordinated azides on a mononuclear precursor,<sup>18,19</sup> by metathesis with reagents such as  $(Me_3Sn)_3N$ ,<sup>20</sup> by reduction of nitrosyl ligands appended to iron carbonyl clusters,<sup>21</sup> or by reduction of dinitrogen (Scheme 2).<sup>9</sup> Aside from nitrosyl reduction, these methods rely on the self-assembly of monometallic precursors, with the only exception being spontaneous decomposition of azide at room temperature by a triiron(II) cluster.<sup>22</sup> Few systems have the requisite control of nuclearity, of the spatial and electronic parameters of the clusters, and of the modularity to methodically vary the bridging ligand. We have previously demonstrated that sulfide can be readily installed in our tricopper system by reaction with  $S_8$ ,<sup>23a</sup> which suggested that general routes may exist to vary the interstitial ligands within this cluster type.

Under the first aim of investigating and harnessing the redox cooperativity, we reported that the reaction of a triiron(II) cluster,  $Fe_3Br_3L$  (**1**), with  $KC_8$  under a dinitrogen atmosphere results in the cleavage of dinitrogen to afford protonated N-atom bridges.<sup>23b</sup> One surprising aspect of this system is the incorporation of three N-atom ligands per cluster. This result indicates that 1 equiv of dinitrogen is likely cleaved at the interface of two triiron complexes in at least one step in the overall reaction. This assertion is supported by the crystal structure of a dimeric species in which two  $K^+$  cations bridge two clusters, which demonstrates that the close approach of two triiron complexes is feasible. However, this intercluster or dimer mechanism could be the sole pathway by which the substrate is activated in this system; that is, the reduction of each equiv of dinitrogen requires the participation of six Fe centers (Scheme 3). If such an intercluster-only mechanism operates, one could envision that (i) an initial product would be a nitride-bridged cluster and (ii) complete or partial dissociation of the dimer would be required to allow for cluster rearrangement and/or coordination of the subsequent equivalents of dinitrogen. Independent of that mechanistic question, we were also drawn to understanding how a central atom donor tunes the reduction potential of the cluster and dictates the interplay between dinitrogen coordination versus

Scheme 3

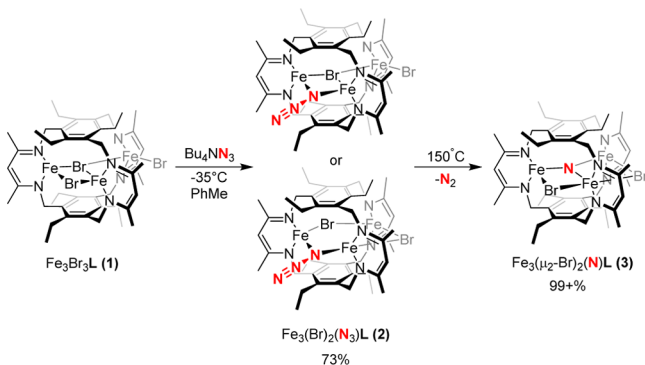


activation. Toward that goal, we report the synthesis and characterization of a nitride-bridged triiron cluster and, specifically, the redox properties of this complex compared to those of the previously reported triiron(II) triamide complex.

## RESULTS AND DISCUSSION

The reaction of 1 equiv of tetrabutylammonium azide with a toluene solution of  $\text{Fe}_3\text{Br}_3\text{L}$  (**1**) at  $-35^\circ\text{C}$  yielded the monoazide complex  $\text{Fe}_3(\text{Br})_2(\text{N}_3)\text{L}$  (**2**) as a pale-red solid in good yield (73%; Scheme 4). Substitution of the halide for azide

Scheme 4



azide was readily apparent by IR spectroscopy because an intense absorption at  $2082\text{ cm}^{-1}$  appears during the course of the reaction. This absorption is at comparable energy to the vibration assigned to metal-bound azides including the di( $\mu$ -1,3-azido)diiron(II) clusters reported by Peters and Holland.<sup>18a,19,24</sup> In addition, combustion analysis supports the proposed formula of **2**. Evaporation of a benzene solution afforded single crystals of **2**, which were suitable for X-ray diffraction studies. In the molecular structure, we observe significant disorder in the structure, which will be discussed in greater detail below; however, density consistent with an azide donor coordinated in a  $\mu$ -1,1 manner to two Fe centers is evident. Although the data set is of sufficient quality for a structure solution, the extent of disorder precludes a detailed comparison of the bond metrics compared to other azide-ligated metal complexes. To our knowledge, there are few examples of an all-ferrous cluster with a bridging azide donor;<sup>24f,h,25</sup> a number of these compounds undergo spontaneous loss of dinitrogen to afford the nitride or a downstream product. Indeed, the facile substitution of only one

bromide for an azide without concomitant N–N bond cleavage provides a facile route to vary the bridging ligand or to install additional donors.

Heating a solid sample of **2** at  $150^\circ\text{C}$  under an inert atmosphere affords a new species **3** in quantitative yield. By IR spectroscopy, a gradual decrease and ultimate disappearance of the absorption at  $2082\text{ cm}^{-1}$  occurs concomitantly with an increase in the intensity of a new feature at  $627\text{ cm}^{-1}$ . The latter absorption is higher in energy than that assigned as the  $\nu_{\text{as}}(\text{M}_3\text{O})$  mode in mixed-valent oxo-bridged triiron(II/III/III) complexes (e.g., 530 and  $582\text{ cm}^{-1}$ ).<sup>26</sup> This difference likely arises from the expected stronger bond strength for Fe–N compared to Fe–O bonds, which is supported by the relative energies of  $\nu(\text{FeN})$  versus  $\nu(\text{FeO})$  in tetraphenylporphyrin complexes<sup>27</sup> and the lower coordination number of the Fe centers in **3** compared to the oxo-bridged compounds. The  $627\text{ cm}^{-1}$  band is lower in energy than that for the  $\text{Fe}^{\text{III}}\text{–N–Fe}^{\text{IV}}$  vibration in ( $\mu$ -nitrido)bis(tetraphenylporphyrinato)diiron(III/IV);<sup>27a</sup> however, this difference is expected given the higher oxidation states of metal centers in the porphyrin complex. Similar trends are observed in the UV–visible absorption spectra of **2** and **3**. For benzene solutions of **2**, there is an absorption maximum at 308 nm [ $\epsilon_{308} = 3.60(5) \times 10^4\text{ M}^{-1}\text{ cm}^{-1}$ ] with shoulders at 399, 420, and 542 nm [ $\epsilon_{399} \sim 1.27(2) \times 10^4\text{ M}^{-1}\text{ cm}^{-1}$ ,  $\epsilon_{420} \sim 1.37(2) \times 10^4\text{ M}^{-1}\text{ cm}^{-1}$ , and  $\epsilon_{542} \sim 2.3(1) \times 10^3\text{ M}^{-1}\text{ cm}^{-1}$ , respectively]. The values of  $\lambda_{\text{max}}$  and  $\epsilon$  are comparable to those of the mononuclear iron(II) azides reported previously.<sup>18a,24b</sup> There are marked changes to the spectrum after heating **2**, such as the loss of absorption at 542 nm, with new  $\lambda_{\text{max}}$  values of 322 nm ( $\epsilon_{322} \sim 2.40(15) \times 10^4\text{ M}^{-1}\text{ cm}^{-1}$ ) and 423 nm ( $\epsilon_{423} \sim 2.4(4) \times 10^3\text{ M}^{-1}\text{ cm}^{-1}$ ) observed for solutions of **3**. In particular, the low-energy feature in **3** at 423 nm is of similar energy and has an extinction coefficient comparable to those reported for other nitride-bridged polynuclear iron clusters.<sup>18b,20,22</sup> Although there are few direct comparisons based on the oxidation state and coordination environment of the clusters in **2** and **3**, the spectroscopic data are consistent with thermal decomposition of the azide ligand in **2** to afford complex **3**.<sup>22</sup>

In addition to the IR and UV–visible absorption data, the solution-state magnetic susceptibilities for **3** ( $3.09\ \mu_{\text{B}}$ ) and **2** ( $5.07\ \mu_{\text{B}}$ ) in toluene as determined by Evans' method differ significantly and support a two-electron oxidation of **3** compared with **2**.<sup>28</sup> This decrease in the susceptibility arises from the expected stronger antiferromagnetic coupling between  $\text{Fe}^{\text{III}}$  centers compared to  $\text{Fe}^{\text{II}}$  ions. We have observed similar trends between iron(II) and iron(III) clusters supported by our ligand.<sup>29,30</sup> In agreement with a mixed-valent complex, a weak and broad absorption is observed in near-IR (NIR) spectra of solutions of **3** with  $\lambda_{\text{max}} = 1117\text{ nm}$ . This feature is comparable to the intervalence charge-transfer band reported for the mixed-valent  $\text{Fe}^{\text{III}}\text{–N–Fe}^{\text{II}}$  reported by Brown et al.<sup>18</sup>

To validate the inclusion of an N atom within the cluster, we conducted protonolysis of **3**, followed by quantification of the released nitrogen-containing ligand by the indophenol method.<sup>9,31</sup> The ammonia generated upon acid decomposition of **3** was lower ( $35 \pm 1\%$ ) than expected for one nitride ligand per complex. However, the yields on  $\text{NH}_3$  using this assay on the product of reduction of **1** with  $\text{KC}_8$  under dinitrogen (**5**) and on the tri- $\mu_2$ -amidotriiron(II) complex (**4**) were also significantly lower than expected.<sup>23b</sup> We attributed these previously reported low ammonia yields to incomplete release of N-atom donors from the cluster under the assay conditions,

and a similar effect may occur for **3**. Taken together then, our results are consistent with **3** assigned as  $\text{Fe}_3(\text{Br})_2(\text{N})\text{L}$ , which agrees with prior reports of thermal decomposition of transition-metal azides to liberate dinitrogen and afford the corresponding metal nitride species. This formulation is supported by high-resolution mass spectrometry data, in which ions such as  $[\text{M} - 2\text{Br} + \text{Cl}]^+$ —chloride arises from trace contamination in the instrument lines—and  $[\text{M} - 2\text{Br}]^+$  are observed in the spectrum (Figures S9 and S10 in the SI), as well as combustion analysis results. Compound **3** constitutes one of a growing but still uncommon family of midvalent iron nitride compounds and one of two designed multinuclear iron nitride clusters.<sup>18,22</sup>

As alluded to above, the molecular structure determined from single crystals of **2** is disordered, albeit in an unexpected manner. The cyclophane ligand in the structure is well resolved with minimal disorder, and the disorder is localized to the cluster itself. In the higher-occupancy part in the structure solution, Fe1, Fe2, Fe3, and Br1 were readily modeled with occupancies of 85%, whereas Br2 required a slightly lower value (75%) to adequately model the electron density. We do not observe density consistent with an azide ligand with similar percent occupancies, but instead a central atom donor, X, is present. Initially, we treated X as a bromide, reasoning that this ligand could arise from either the incomplete substitution of one  $\text{Br}^-$  ligand in **1** upon the addition of  $[\text{Bu}_4\text{N}]\text{N}_3$  or from different structural isomers of **2** (Scheme 4). For example, the substitution of one bromide could retain the central bromide to yield  $\text{Fe}_3(\mu_2\text{-N}_3)(\mu_3\text{-Br})(\mu_2\text{-Br})\text{L}$  or result in a minor structural rearrangement to afford  $\text{Fe}_3(\mu_2\text{-N}_3)(\mu_2\text{-Br})_2\text{L}$  (Scheme 4). The X ligand, however, refined poorly as  $\text{Br}^-$  even when the occupancy was varied, and, more importantly, the observed Fe–X distances (2.022–2.166 Å) were significantly shorter than the Fe–Br distances reported for **1** (i.e., 2.470–2.586 Å).<sup>30</sup> Instead of bromide then, we modeled the central atom as a N atom and the quality of the structure solution improved significantly, with the final solution treating the central atom as a mixture of N (85%) and Br (15%). Therefore, we formulate the major species in the structural solution as containing a central nitride donor. This result suggests either that **2** decomposes to **3** in the solid state under X-ray irradiation during data collection or that crystalline “**2**” is not homogeneous but exists as a mixture of the monoazide complex and **3**. For the former, alkali and main-group azides are known to undergo decomposition upon X-ray irradiation,<sup>32</sup> but the plethora of crystal structures of azide-bridged multinuclear transition-metal compounds indicates that decomposition should be unlikely during X-ray data collection. For the latter, decomposition could occur either in the reaction mixture or during crystallization at room temperature. Betley and co-workers reported the reaction of a high-spin triiron(II) cluster with azide, which spontaneously affords the anionic nitride complex under ambient conditions.<sup>22</sup> The Fe–N bond distances in that species were significantly shorter (1.871 Å) than the ones that we observe here, but that discrepancy could arise from either the disorder or the different structural constraints placed on the cluster by our ligand compared to theirs. We do not observe changes to the relative intensity of the azide vibration compared to other ligand-based modes in the as-isolated versus crystallized sample, suggesting that minimal decomposition, if any, occurs during crystallization or is likely at the reduced temperature used for the synthesis. Previously, the crystal structure of a dimeric di( $\mu$ -1,3-azido)-

bis[( $\beta$ -diketiminato)iron(II)] complex was reported,<sup>24h</sup> and the Fe centers in that compound are anticipated to have reactivities somewhat similar to those of the compound reported here. The minimal structural rearrangement required in **2** compared to that in the monometallic analogue could facilitate more facile loss of dinitrogen, as is suggested by the fact that the aforementioned diazide does not undergo thermolysis.<sup>33</sup> Finally, we do not observe changes to the crystal morphology or color that suggest oxidation of the compound; exposure of **1–3** to air results in an immediate color change to afford greenish-black solutions.

One metric that we have previously used to evaluate distortion in complexes of this ligand is the dihedral angle between the two arene rings of the triethylbenzene caps. This angle is  $\sim 7^\circ$ , which is larger than that observed for any reported complex of this ligand.<sup>23,30,34</sup> In addition, the average Fe–Br bond distance is also longer than that in **1**, and the N···N distances in each nacnac arm (e.g., N5–N6 or N1–N2) are also shorter than those in **1**.<sup>30</sup> The observed distortions in the structure might arise from a steric clash between the halide and the Et substituents as the central donor atom decreases in size and the cluster oxidation state increases. Although  $\text{N}_3^-$  is not present in the highest-occupancy structural solution, the electron density consistent with a  $\mu$ -1,1-azide ligand is observed with lower partial occupancy (15%) in the structure (Figure 1).

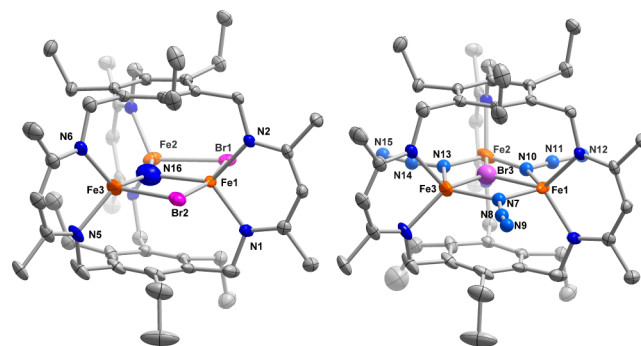
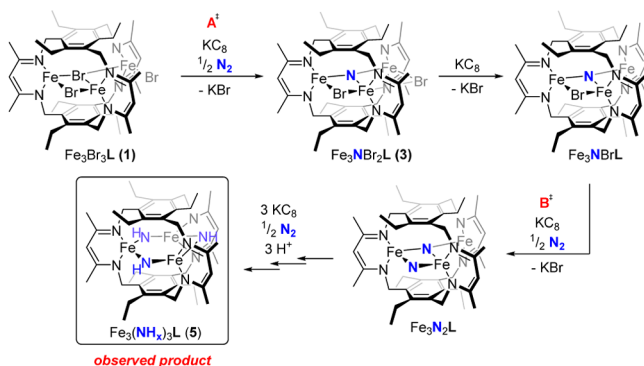


**Figure 1.** Structure solutions for X-ray diffraction data collected on crystals of **2**. The cluster core is disordered, with the higher-occupancy part best modeled as having two bromide and one nitride ligands (left). The occupancies for Fe1–3, Br1, and N16 are 85%, whereas that of Br2 is 75%. The central atom is partly modeled as a central Br (15%), and the azide ligand is disordered over all three bridging positions (15%) in the minor-occupancy part of the solution (right). C, N, Br, and Fe atoms are depicted as gray, blue, purple, and orange ellipsoids at the 50% probability level, respectively. The partially occupied azide N atoms and the central Br atom in the lower-occupancy solution are depicted as spheres of standard radii. H atoms are omitted for clarity.

This pseudohalide is disordered over each of the three possible  $\mu_2$  sites in the complex. Although the density modeled as the  $\mu_2$ -bromide ligands in the higher-occupancy part of the solution is nearly coincident with that of the central N atom in two of the azide ligands, the two remaining N atoms in the  $\text{N}_3^-$  ligand are readily observed. Finally, minor disorder is also observed for the Fe atoms, which corresponds to minor displacements of the Fe centers out of the NCCCN plane of the bound diketiminato arm. Similar positional disorder in the metal centers has been reported previously for **1**, as well as the manganese analogue  $\text{Mn}_3\text{Br}_3\text{L}$  and  $\text{Cu}_3(\text{N}_2)\text{L}$ .<sup>30,34b</sup>

Chemical reduction of **1** resulted in the incorporation of three dinitrogen-derived ligands in the isolated product (**5**), which suggested that both an intracluster and an intercluster mechanism could be involved with the latter required for the activation of at least 1 equiv of dinitrogen (Scheme 5).<sup>23b</sup>

Scheme 5



† Steps **A** and **B** require formation of a dimer

Mechanistically, however, one could envision that an intercluster mechanism could be the predominant pathway for the cleavage of 3 equiv of dinitrogen. In this intercluster-only mechanism, one- or two-electron reduction of **1** could generate triiron complexes with sufficient reactivity to cooperatively cleave dinitrogen between two triiron complexes. Thus, we expected that triiron clusters containing one or two bromide donors and one nitride would be plausible intermediates in this pathway. In addition, we reported that only  $\text{Fe}_3(\text{NH}_x)_3\text{L}$  ( $x = 1$  or  $2$ ) and unreacted **1** were isolated in reduction reactions carried out under a dinitrogen atmosphere with less than 6 equiv of  $\text{KC}_8$ .<sup>23b</sup> We speculated that this product distribution would be possible if early dinitrogen reduction products were more readily reduced than **1**, which would funnel reducing equivalents to generate the isolated product  $\text{Fe}_3(\text{NH}_x)_3\text{L}$ . By this argument, the redox properties of an authentic nitride-bridged triiron cluster should provide insight into the mechanism of dinitrogen activation by **1**. Simply, an intercluster-only mechanism starting from dinitrogen cleavage by the one-electron-reduced analogue of **1** [i.e.,  $\text{Fe}_3(\text{Br})_2\text{L}$ ] is unlikely if **3** is more difficult to reduce than **1** because **1** would be preferentially reduced compared to this intermediate. One assumption in our mechanistic approach is that dimeric clusters dissociate after dinitrogen bond scission and large hexairon species are transient in the reaction. Thus, we examined the redox properties of **3** as well as the triamide complex synthesized by salt metathesis,  $\text{Fe}_3(\text{NH}_2)_3\text{L}$  (**4**).

Cyclic voltammograms of **2**–**4** were recorded in isobutyronitrile at ambient temperature. Broad irreversible reductive waves are present at  $-0.28$ ,  $-2.20$ , and  $-2.50$  V versus  $\text{Fc}/\text{Fc}^+$  in the voltammogram for **2** with similarly irreversible features at  $-0.06$  and  $1.00$  V in the oxidative scan (Figure S6 in the SI). After conversion of **2** to **3** and associated oxidation of the cluster, however, these features are no longer observed, but the data are very similar to those reported for **1**; we do not observe reductive or oxidative waves between 0 and  $-2.50$  V (Figure 2). We were initially surprised by these data because other nitride- and imide-bridged polynuclear mid- and high-valent iron compounds have reversible reductions ranging from  $-0.20$  to  $-2.54$  V versus  $\text{Fc}/\text{Fc}^+$ .<sup>18,21a,35</sup> Notwithstanding, the absence of

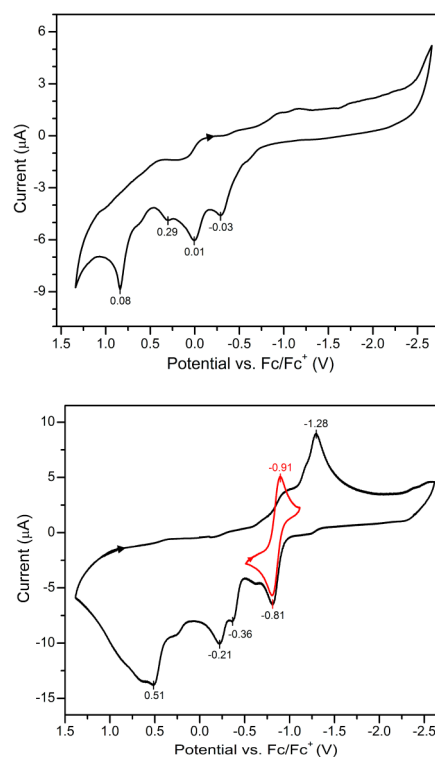


**Figure 2.** Cyclic voltammograms of **3** (top) and **4** (bottom) in isobutyronitrile at a scan rate of  $100 \text{ mV}\cdot\text{s}^{-1}$ . There are no reductive waves observed for **3** from  $\sim 0$  to  $-2.5$  V. In contrast, a broad redox couple is present at  $E_{1/2} = -0.86$  V for **4**. The behavior of the reductive wave is more complex than that of the oxidative wave, suggesting an EC or ECE process.

any reductive waves is striking and suggests that the intercluster-only mechanism—at least, starting with one-electron reduction of **1**—is unlikely for our triiron complexes. Chemical reduction with strong reducing agents, such as the reaction of **1** with  $\text{KC}_8$  under dinitrogen, may not necessarily correlate with the cyclic voltammetry (CV) data, given the differences in the experimental conditions. Preliminary results from the reduction of **3** with  $\text{KC}_8$ , however, support our conclusion because we observe no evidence for atmospheric dinitrogen reduction by **3**.<sup>36</sup> In initial scans over a broad potential window for **4**, we observed several oxidative events in the range of  $-0.81$  to  $+0.51$  V as well as a reductive wave at  $-1.26$  V with a noticeable shoulder at  $-0.91$  V (Figure 2, bottom, black trace). In particular, the richer reductive chemistry of **4** was somewhat surprising, and we subsequently attempted to correlate the oxidative events to these reductions. Narrowing the scan window, we were able to isolate a reversible one-electron redox event with  $E_{1/2} = -0.84$  V, as confirmed by the linear dependence for  $\nu^{1/2}$  versus both  $i_{pc}$  and  $i_{pa}$  over a range of scan rates by CV and the  $\sim 102$  mV width at half-maximum in differential pulse voltammograms (Figures S7 and S8 in the SI). There are few reports detailing the electrochemical properties of amido-bridged iron clusters to compare with those of **4**; however, iron amide complexes have been proposed as intermediates in the catalytic reduction of dinitrogen,<sup>3b,7,37</sup> an independently synthesized amidoiron complex can be reduced and protonated to liberate  $\text{NH}_3$ , and the resultant complex binds dinitrogen.<sup>38</sup> In this latter case, the authors reported that reversible reductions were not observed over the potential window, which contrasts with that observed

for **4**. Reductive waves at potentials comparable to those in the CV of **4** were observed for a related diiron complex containing two  $\mu_2$ -amide and one  $\mu$ -1,2-diazene ligands, although the nature of that reduction (e.g., ligand- or metal-based) is unclear.<sup>39</sup> Similar downstream reactions upon reduction could occur for **4**, which would afford voltammograms similar to ECE mechanisms.<sup>40</sup> Although more detailed characterization including isolation of the reduced congeners of **4** is required, an ECE mechanism seems plausible when one considers the change in the peak current in scans encompassing both the  $-1.28$  V reductive wave and the reversible process. This result provides an interesting proposition that abstraction of the  $\text{NH}_2^-$  ligands could be possible in the presence of an appropriate acceptor, allowing for more than one turnover in the reaction.

## CONCLUSIONS

In conclusion, we report the synthesis of two triiron complexes, one in which an azide ligand is introduced by salt metathesis (**2**) and the other that arises from decomposition of the installed  $\text{N}_3^-$  to afford a bridging nitride donor (**3**). Complex **3** is an uncommon example of a mid-valent nitridotriiron cluster and, in particular, represents only the second example of the targeted synthesis of such a cluster using a ligand design approach. Contrary to our expectations, there are no reversible redox processes observed for **3**, and no reductions are evident up to  $-2.50$  V. The result suggests that this species is unlikely to be the dominant on-pathway mechanism for dinitrogen reduction by **1** and implies that intracenter redox cooperative steps, in which three Fe centers in one cluster cleave the first equiv of  $\text{N}_2$  is an early step in dinitrogen activation in this system. Moreover, **3** provides a starting point toward the synthesis of other potential intermediates, such as  $(\mu_2\text{-nitrido})(\mu_3\text{-nitrido})$ triiron clusters, and evaluation of the reactivities and properties of these species. The syntheses of **2** and **3**, as well as other trimetallic complexes of our ligand-containing central atom donors, provide evidence that a general and systematic approach can be taken to evaluate the role of interstitial atoms on reactivity.

## EXPERIMENTAL SECTION

**General Considerations.** All reactions were performed under a dinitrogen atmosphere in an Innovative Technologies glovebox. Solvents were purchased from Sigma-Aldrich, then dried using an Innovative Technologies solvent purification system, and stored over activated 3 Å molecular sieves.  $\text{FeBr}_2$  was purchased from Acros and first dried under a dinitrogen stream at  $150$  °C and then under vacuum. Tetrabutylammonium azide was either purchased from Sigma-Aldrich, recrystallized from cold toluene, and dried over  $\text{P}_2\text{O}_5$ , or synthesized as described elsewhere.<sup>41</sup> **Caution!** Azides are potentially explosive and should be handled with care. Deuterated solvents were purchased from Cambridge Isotope Laboratories, dried, and then stored over activated 3 Å molecular sieves using the procedures reported for the corresponding protonated solvents.<sup>42</sup> NMR spectra were collected on a Varian Inova (500 MHz) or a Mercury (300 MHz) spectrometer equipped with a three-channel 5 mm indirect detection probe with  $z$ -axis gradients. All chemical shifts are reported in parts per million (ppm) and referenced to tetramethylsilane for  $^1\text{H}$  and  $^{13}\text{C}$  NMR. UV–visible–NIR absorption spectra were collected using a Varian Cary 50 spectrophotometer and quartz cuvettes having a 1 cm path length and air-free screw top seal (Starna Cells Inc., Atascadero, CA). Longer-wavelength NIR spectra were recorded on a PerkinElmer Lambda 800/900 UV–vis–NIR spectrometer, purged with nitrogen, using UV Winlab<sup>TM</sup> software at a  $4\text{ nm}\cdot\text{s}^{-1}$  scan rate. IR spectra were collected in a nitrogen-filled glovebox using a Bruker Alpha with an ATR diamond crystal stage using the Opus 7.0 software package.

Complete Analysis Laboratories, Inc. (Parsippany, NJ) conducted elemental analyses on samples shipped under vacuum in flame-sealed ampules.  $\text{H}_3\text{L}$ ,  $\text{Fe}_3\text{Br}_3\text{L}$  (**1**), and  $\text{Fe}_3(\text{NH}_2)_3\text{L}$  (**4**) were synthesized as described previously.<sup>23b,30</sup> Cyclic and differential pulse voltammograms were recorded on a Princeton Applied Research Versastat II potentiostat and a three-electrode setup using a 2 mm platinum button working electrode, a  $\text{Ag}/\text{AgNO}_3$  in acetonitrile reference electrode, and a gold coil counter electrode (purchased from BASi, Inc., and/or CH Instruments, Inc.) in isobutyronitrile with 0.3 M  $\text{Bu}_4\text{NPF}_6$  as the electrolyte. Electrospray ionization mass spectrometry (ESI-MS) spectra were collected by direct injection into an Agilent 6120 TOF spectrometer at a gas temperature of  $350$  °C and a fragmentation voltage of  $120$  V on solution samples prepared in a nitrogen atmosphere glovebox and transported in Hamilton gastight sample-lock syringes.

**X-ray Crystallography.** X-ray intensity data were collected at  $100$  K on a Bruker DUO diffractometer using  $\text{Mo K}\alpha$  radiation ( $\lambda = 0.71073$  Å) and an APEXII CCD area detector. Raw data frames were read by the program SAINT<sup>43</sup> and integrated using 3D profiling algorithms. The resulting data were reduced to produce  $hkl$  reflections and their intensities and estimated standard deviations. The data were corrected for Lorentz and polarization effects, and numerical absorption corrections were applied based on indexed and measured faces. The structure was solved and refined in SHELXTL2014,<sup>44</sup> using full-matrix least-squares refinement. The non-H atoms were refined with anisotropic thermal parameters, and all of the H atoms were calculated in idealized positions and refined riding on their parent atoms. The asymmetric unit consists of the triiron complex and one benzene solvent molecule in general positions and two half-molecules located on inversion centers. The structure has significant disorder in the core of the complex involving all three Fe centers and the Br and azide ligands. Although each Fe center is refined in two positions, the Br ligands are disordered against the azide ligands. Along with the N13–14–15 azide ligand, there is a disorder in the C30–31/C30'–31' ethyl arm of the molecule. In the model where the core consists of the Fe and Br positions disordered over two positions, there exists a density best modeled as a nitride ligand, N16, which does not exist in the model that has the azide ligands. In summary, the structure of is an average of complexes with azide/Br disordered in the three  $\mu_2$ -bridging positions forming, along with the three disordered Fe centers, affording a hexagonal  $\text{Fe}_3\text{X}_3$  cluster, and complexes containing a nitride ligand at the core center. The azide ligands were constrained to maintain all angles to be equivalent using the SADI command in the SHELX refinement. The minor part of the disorder has the Fe atoms refined with equivalent displacement parameters using the EADP command. In the final cycle of refinement, 12398 reflections [of which 7926 are observed with  $I > 2\sigma(I)$ ] were used to refine 678 parameters, and the resulting R1, wR2, and S (goodness of fit) were 5.67%, 13.63%, and 1.026, respectively. The refinement was performed by minimizing the wR2 function using  $F^2$  rather than  $F$  values. R1 was calculated to provide a reference to the conventional  $R$  value, but its function is not minimized.

**Synthesis of  $\text{Fe}_3(\text{Br})_2(\text{N}_3)\text{L}$  (**2**).** Tetrabutylammonium azide (129 mg, 0.457 mmol) was added slowly to a solution of **1** (476 mg, 0.434 mmol) in toluene (15 mL) at  $-35$  °C and the reaction stirred overnight at  $-35$  °C. The reaction was then filtered through a fine-fritted glass funnel packed with a Celite plug, the residue was washed with toluene ( $\sim 15$  mL), and the combined filtrates were dried under reduced pressure to yield **2** as a pale-red solid (335 mg, 73%). Combustion analysis on as-isolated **2**,  $\text{C}_{45}\text{H}_{63}\text{Br}_2\text{Fe}_3\text{N}_9$  (calcd): C, 50.99 (51.12); H, 5.95 (6.01); N, 11.78 (11.92). IR ( $\text{cm}^{-1}$ ):  $\nu(\text{N}_3)$  2082.  $\mu_{\text{eff}} = 5.07 \mu_{\text{B}}$ . X-ray-quality crystals were grown from the slow evaporation of a saturated benzene solution into immersion oil at room temperature.

**Synthesis of  $\text{Fe}_3(\text{Br})_2(\text{N})\text{L}$  (**3**).** **2** (121 mg, 0.114 mmol) was placed in a 20 mL vial and heated at  $150$  °C for 24 h, during which the solid changed color from pale red to olive green (117 mg, >99%). Combustion analysis on **3**,  $\text{C}_{45}\text{H}_{63}\text{Br}_2\text{Fe}_3\text{N}_7$  (calcd): C, 52.42 (52.51); H, 6.00 (6.17); N, 9.37 (9.52). IR ( $\text{cm}^{-1}$ ):  $\nu(\text{Fe}_3\text{--N})$  627.  $\mu_{\text{eff}} = 3.09 \mu_{\text{B}}$ .

**Indophenol Assay.** This test was carried out on samples of **3**, which were prepared using the general procedure outlined below and reported previously.<sup>9</sup> To a frozen solution of **3** (4.0 mg, 3.9  $\mu\text{mol}$ ) was added HCl in diethyl ether (2.0 M, 200  $\mu\text{L}$ , 0.40 mmol), which resulted in an immediate color change from olive green to light yellow. The mixture was warmed to room temperature and stirred overnight, after which all volatiles were removed under reduced pressure. The pale-yellow residue was dissolved in a phosphate buffer (5 mL, 50 mM, pH 6.94), filtered through a fine-fritted glass funnel packed with Celite, the residue was washed with deionized water (3  $\times$  1 mL), and the filtrate was diluted to 10 mL with deionized water in a volumetric flask. Ammonia was quantified using the indophenol method as previously published.<sup>31</sup>

## ■ ASSOCIATED CONTENT

### ■ Supporting Information

X-ray crystallographic data in CIF format, additional spectroscopic data, including NIR, IR, NMR, and ESI-MS spectra, voltammetry, and crystallographic details. The Supporting Information is available free of charge on the ACS Publications website at DOI: 10.1021/acs.inorgchem.5b00825.

## ■ AUTHOR INFORMATION

### Corresponding Author

\*E-mail: murray@chem.ufl.edu.

### Author Contributions

The manuscript was written through contributions of all authors.

### Notes

The authors declare no competing financial interest.

## ■ ACKNOWLEDGMENTS

The following institutions are acknowledged: NSF for a CRIF award to the University of Florida (UF) Chemistry Department (Grant CHE-1048604 to L.J.M.); NSF (Grant CHE-0821346) and UF for funding an X-ray equipment purchase (K.A.A.); UF (L.J.M. and K.A.A.); ACS Petroleum Research Fund 52704-DNI3 and NSF (Grant CHE-1464876 to L.J.M.); a fellowship from UF College of Liberal Arts and Sciences Graduate School (D.E.); UF Center for Undergraduate Research (J.B.G.). The authors thank Prof. A. Rinzler and Dr. S. Vasileva (UF, Physics) for the use of and help collecting data on their NIR spectrophotometer and Y. Lee for help with the artwork.

## ■ REFERENCES

- (1) Bazhenova, T. A.; Shilov, A. E. *Coord. Chem. Rev.* **1995**, *144*, 69.
- (2) *Ullmann's Encyclopedia of Industrial Chemistry*, 7th ed.; John Wiley & Sons, Inc.: Weinheim, Germany, 2005.
- (3) (a) Hoffman, B. M.; Lukoyanov, D.; Yang, Z.-Y.; Dean, D. R.; Seefeldt, L. C. *Chem. Rev.* **2014**, *114*, 4041. (b) Burgess, B. K.; Lowe, D. J. *Chem. Rev.* **1996**, *96*, 2983.
- (4) Laplaza, C. E.; Cummins, C. C. *Science* **1995**, *268*, 861.
- (5) Yandulov, D. V.; Schrock, R. R. *Science* **2003**, *301*, 76.
- (6) (a) Arashiba, K.; Miyake, Y.; Nishibayashi, Y. *Nat. Chem.* **2011**, *3*, 120. (b) Nishibayashi, Y.; Iwai, S.; Hidai, M. *Science* **1998**, *279*, 540. (c) Tanaka, H.; Arashiba, K.; Kuriyama, S.; Sasada, A.; Nakajima, K.; Yoshizawa, K.; Nishibayashi, Y. *Nat. Commun.* **2014**, *5*, 3737. (d) Yuki, M.; Tanaka, H.; Sasaki, K.; Miyake, Y.; Yoshizawa, K.; Nishibayashi, Y. *Nat. Commun.* **2012**, *3*, 1254. (e) Miyazaki, T.; Tanaka, H.; Tanabe, Y.; Yuki, M.; Nakajima, K.; Yoshizawa, K.; Nishibayashi, Y. *Angew. Chem., Int. Ed.* **2014**, *53*, 11488.
- (7) Lukoyanov, D.; Dikanov, S. A.; Yang, Z.-Y.; Barney, B. M.; Samoilova, R. I.; Narasimhulu, K. V.; Dean, D. R.; Seefeldt, L. C.; Hoffman, B. M. *J. Am. Chem. Soc.* **2011**, *133*, 11655.

(8) Gilbertson, J. D.; Szymczak, N. K.; Tyler, D. R. *J. Am. Chem. Soc.* **2005**, *127*, 10184.

(9) Rodriguez, M. M.; Bill, E.; Brennessel, W. W.; Holland, P. L. *Science* **2011**, *334*, 780.

(10) (a) MacLeod, K. C.; Vinyard, D. J.; Holland, P. L. *J. Am. Chem. Soc.* **2014**, *136*, 10226. (b) Figg, T. M.; Holland, P. L.; Cundari, T. R. *Inorg. Chem.* **2012**, *51*, 7546. (c) Grubel, K.; Brennessel, W. W.; Mercado, B. Q.; Holland, P. L. *J. Am. Chem. Soc.* **2014**, *136*, 16807.

(11) (a) Lee, Y.; Mankad, N. P.; Peters, J. C. *Nat. Chem.* **2010**, *2*, 558. (b) Saouma, C. T.; Peters, J. C. *Coord. Chem. Rev.* **2011**, *255*, 920. (c) Hendrich, M. P.; Gunderson, W.; Behan, R. K.; Green, M. T.; Mehn, M. P.; Betley, T. A.; Lu, C. C.; Peters, J. C. *Proc. Natl. Acad. Sci. U. S. A.* **2006**, *103*, 17107.

(12) Rittle, J.; McCrory, C. C. L.; Peters, J. C. *J. Am. Chem. Soc.* **2014**, *136*, 13853.

(13) (a) Kim, J.; Rees, D. C. *Nature* **1992**, *360*, 553. (b) Kim, J.; Rees, D. C. *Science* **1992**, *257*, 1677.

(14) (a) Einsle, O.; Tezcan, F. A.; Andrade, S. L. A.; Schmid, B.; Yoshida, M.; Howard, J. B.; Rees, D. C. *Science* **2002**, *297*, 1696. (b) Dance, I. *Chem. Commun.* **2003**, 324. (c) Lee, H.-I.; Benton, P. M. C.; Laryukhin, M.; Igarashi, R. Y.; Dean, D. R.; Seefeldt, L. C.; Hoffman, B. M. *J. Am. Chem. Soc.* **2003**, *125*, 5604. (d) Hinnemann, B.; Nørskov, J. K. *J. Am. Chem. Soc.* **2003**, *125*, 1466.

(15) (a) Lancaster, K. M.; Roemelt, M.; Ettenhuber, P.; Hu, Y.; Ribbe, M. W.; Neese, F.; Bergmann, U.; DeBeer, S. *Science* **2011**, *334*, 974. (b) Spatzal, T.; Aksoyoglu, M.; Zhang, L.; Andrade, S. L. A.; Schleicher, E.; Weber, S.; Rees, D. C.; Einsle, O. *Science* **2011**, *334*, 940. (c) Wiig, J. A.; Hu, Y.; Lee, C. C.; Ribbe, M. W. *Science* **2012**, *337*, 1672.

(16) Pollock, C. J.; Tan, L. L.; Zhang, W.; Lancaster, K. M.; Lee, S. C.; DeBeer, S. *Inorg. Chem.* **2014**, *53*, 2591.

(17) Lee, S. C.; Holm, R. H. *Proc. Natl. Acad. Sci. U. S. A.* **2003**, *100*, 3595.

(18) (a) Brown, S. D.; Peters, J. C. *J. Am. Chem. Soc.* **2005**, *127*, 1913. (b) Brown, S. D.; Mehn, M. P.; Peters, J. C. *J. Am. Chem. Soc.* **2005**, *127*, 13146.

(19) (a) Summerville, D. A.; Cohen, I. A. *J. Am. Chem. Soc.* **1976**, *98*, 1747. (b) Wagner, W.-D.; Nakamoto, K. *J. Am. Chem. Soc.* **1988**, *110*, 4044. (c) Meyer, K.; Bill, E.; Mienert, B.; Weyhermüller, T.; Wieghardt, K. *J. Am. Chem. Soc.* **1999**, *121*, 4859. (d) Dutta, S. K.; Beckmann, U.; Bill, E.; Weyhermüller, T.; Wieghardt, K. *Inorg. Chem.* **2000**, *39*, 3355.

(20) Bennett, M. V.; Stoian, S.; Bominaar, E. L.; Münck, E.; Holm, R. H. *J. Am. Chem. Soc.* **2005**, *127*, 12378.

(21) (a) Pergola, R. D.; Garlaschelli, L.; Manassero, M.; Sansoni, M.; Strumolo, D.; de Biani, F. F.; Zanello, P. *J. Chem. Soc., Dalton Trans.* **2001**, 2179. (b) Fjare, D. E.; Gladfelter, W. L. *J. Am. Chem. Soc.* **1981**, *103*, 1572.

(22) Powers, T. M.; Fout, A. R.; Zheng, S.-L.; Betley, T. A. *J. Am. Chem. Soc.* **2011**, *133*, 3336.

(23) (a) Di Francesco, G. N.; Gaillard, A.; Ghiviriga, I.; Abboud, K. A.; Murray, L. J. *Inorg. Chem.* **2014**, *53*, 4647. (b) Lee, Y.; Sloane, F. T.; Blondin, G.; Abboud, K. A.; Garcia-Serres, R.; Murray, L. J. *Angew. Chem., Int. Ed.* **2015**, *54*, 1499.

(24) (a) Abu-Youssef, M. A. M.; Langer, V.; Luneau, D.; Shams, E.; Goher, M. A. S.; Öhrström, L. *Eur. J. Inorg. Chem.* **2008**, *2008*, 112. (b) Goldsmith, C. R.; Jonas, R. T.; Cole, A. P.; Stack, T. D. P. *Inorg. Chem.* **2002**, *41*, 4642. (c) Busetto, L.; Marchetti, F.; Zacchini, S.; Zanotti, V. *Inorg. Chim. Acta* **2005**, *358*, 1204. (d) Tran, B. L.; Krzystek, J.; Ozarowski, A.; Chen, C.-H.; Pink, M.; Karty, J. A.; Telsler, J.; Meyer, K.; Mendiola, D. J. *Eur. J. Inorg. Chem.* **2013**, *2013*, 3916. (e) Scepaniak, J. J.; Young, J. A.; Bontchev, R. P.; Smith, J. M. *Angew. Chem., Int. Ed.* **2009**, *48*, 3158. (f) De Munno, G.; Poerio, T.; Viau, G.; Julve, M.; Lloret, F.; Journaux, Y.; Rivière, E. *Chem. Commun.* **1996**, *22*, 2587. (g) Burrows, A. D.; Dodds, D.; Kirk, A. S.; Lowe, J. P.; Mahon, M. F.; Warren, J. E.; Whittlesey, M. K. *Dalton Trans.* **2007**, 570. (h) Yu, Y.; Sadique, A. R.; Smith, J. M.; Dugan, T. R.; Cowley, R. E.; Brennessel, W. W.; Flaschenriem, C. J.; Bill, E.; Cundari, T. R.;

Holland, P. L. *J. Am. Chem. Soc.* **2008**, *130*, 6624. (i) Sellmann, D.; Hofmann, T.; Knoch, F. *Inorg. Chim. Acta* **1994**, *224*, 61.

(25) (a) De Munno, G.; Poerio, T.; Viau, G.; Julve, M.; Lloret, F. *Angew. Chem., Int. Ed. Engl.* **1997**, *36*, 1459. (b) Escuer, A.; Aromí, G. *Eur. J. Inorg. Chem.* **2006**, *2006*, 4721.

(26) (a) Wu, R.; Poyraz, M.; Sowrey, F. E.; Anson, C. E.; Wocadlo, S.; Powell, A. K.; Jayasooriya, U. A.; Cannon, R. D.; Nakamoto, T.; Katada, M.; Sano, H. *Inorg. Chem.* **1998**, *37*, 1913. (b) Singh, A. K.; Singh, A. K. *Spectrochim. Acta, A: Mol. Biomol. Spectrosc.* **2013**, *112*, 422.

(27) (a) Ercolani, C.; Hewage, S.; Heucher, R.; Rossi, G. *Inorg. Chem.* **1993**, *32*, 2975. (b) Ercolani, C.; Gardini, M.; Monacelli, F.; Pennesi, G.; Rossi, G. *Inorg. Chem.* **1983**, *22*, 2584. (c) Kennedy, B. J.; Murray, K. S.; Zwack, P. R.; Homborg, H.; Kalz, W. *Inorg. Chem.* **1985**, *24*, 3302.

(28) Evans, D. F. *J. Chem. Soc.* **1959**, 2003.

(29) Lee, Y.; Jeon, I.-R.; Abboud, K. A.; García-Serres, R.; Shearer, J.; Murray, L. J. Unpublished results.

(30) Guillet, G. L.; Sloane, F. T.; Ermert, D. M.; Calkins, M. W.; Peprah, M. K.; Knowles, E. S.; Čižmár, E.; Abboud, K. A.; Meisel, M. W.; Murray, L. J. *Chem. Commun.* **2013**, *49*, 6635.

(31) Chaney, A. L.; Marbach, E. P. *Clin. Chem.* **1962**, *8*, 130.

(32) (a) Krause, B. H. *J. Chem. Phys.* **1963**, *39*, 1706. (b) King, G. J.; Carlson, F. F.; Miller, B. S.; McMillan, R. C. *J. Chem. Phys.* **1961**, *34*, 1499. (c) Heal, H. G. *Trans. Faraday Soc.* **1957**, *53*, 210. (d) Carlson, F. F. *J. Chem. Phys.* **1963**, *39*, 1206.

(33) Sadique, A. R.; Holland, P. L. Personal communication.

(34) (a) Ermert, D. M.; Ghiviriga, I.; Catalano, V. J.; Shearer, J.; Murray, L. J. *Angew. Chem., Int. Ed.* **2015**, *54*, 7047. (b) Murray, L. J.; Weare, W. W.; Shearer, J.; Mitchell, A. D.; Abboud, K. A. *J. Am. Chem. Soc.* **2014**, *136*, 13502.

(35) (a) Powers, T. M.; Betley, T. A. *J. Am. Chem. Soc.* **2013**, *135*, 12289. (b) Della Pergola, R.; Bruschi, M.; Fabrizi de Biani, F.; Fumagalli, A.; Garlaschelli, L.; Laschi, F.; Manassero, M.; Sansoni, M.; Zanello, P. C. R. *Chim.* **2005**, *8*, 1850. (c) Della Pergola, R.; Bandini, C.; Demartin, F.; Diana, E.; Garlaschelli, L.; Stanghellini, P. L.; Zanello, P. *J. Chem. Soc., Dalton Trans.* **1996**, 747. (d) Bottomley, L. A.; Gorce, J. N.; Goedken, V. L.; Ercolani, C. *Inorg. Chem.* **1985**, *24*, 3733.

(36) Ermert, D. M.; Abboud, K. A.; Murray, L. J. Unpublished results.

(37) Seefeldt, L. C.; Hoffman, B. M.; Dean, D. R. *Annu. Rev. Biochem.* **2009**, *78*, 701.

(38) Anderson, J. S.; Moret, M.-E.; Peters, J. C. *J. Am. Chem. Soc.* **2013**, *135*, 534.

(39) Sauoma, C. T.; Müller, P.; Peters, J. C. *J. Am. Chem. Soc.* **2009**, *131*, 10358.

(40) Hawley, M. D.; Feldberg, S. W. *J. Phys. Chem.* **1966**, *70*, 3459.

(41) Bates, R. W.; Khanizeman, R. N.; Hirao, H.; Tay, Y. S.; Sae-Lao, P. *Org. Biomol. Chem.* **2014**, *12*, 4879.

(42) Armarego, W. L. F.; Perrin, D. D. *Purification of Laboratory Chemicals*; Butterworth-Heinemann: Oxford, U.K., 1996.

(43) Van der Sluis, P.; Spek, A. L. *Acta Crystallogr., Sect. A* **1990**, *46*, 194.

(44) *SHELXTL*; Bruker AXS: Madison, WI, 2013.